

AD-A117 892

TEXAS UNIV AT AUSTIN DEPT OF CHEMISTRY
PROPERTIES OF PT SUPPORTED ON OXIDES OF TITANIUM. (U)
JUN 82 B CHEN, J M WHITE

F/8 7/4

N00014-75-C-0922

UNCLASSIFIED

TR-23

ML

10/1
10/10/82



END
DATE
FILMED
DTIC

12

OFFICE OF NAVAL RESEARCH
Contract N00014-75-C-0922
Task No. NR 056-578
TECHNICAL REPORT NO. 23

Properties of Pt Supported on Oxides of Titanium
by
Bor-Her Chen and J. M. White

Prepared for publication
in
Journal of Physical Chemistry

Department of Chemistry
University of Texas at Austin
Austin, Texas 78712

June 9, 1982

Reproduction in whole or in part is permitted for
any purpose of the United States Government.

This document has been approved for public release
and sale; its distribution is unlimited.

DTIC
SELECTED

AUG 05 1982

E

AD A117892

DTIC FILE COPY

82 08 05 015

SECURITY CLASSIFICATION OF THIS PAGE (When Data Entered)

REPORT DOCUMENTATION PAGE		READ INSTRUCTIONS BEFORE COMPLETING FORM
1. REPORT NUMBER	2. GOVT ACCESSION NO. AD-A117692	3. RECIPIENT'S CATALOG NUMBER
4. TITLE (and Subtitle) Properties of Pt Supported on Oxides of Titanium	5. TYPE OF REPORT & PERIOD COVERED Technical Report 23 Jan: 1, 1982-Dec. 31, 1982	6. PERFORMING ORG. REPORT NUMBER
		7. AUTHOR(s) Bor-Her Chen and J. M. White
8. CONTRACT OR GRANT NUMBER(s) N00014-75-C-0922	9. PERFORMING ORGANIZATION NAME AND ADDRESS J. M. White Dept. of Chemistry, University of Texas Austin, TX 78712	10. PROGRAM ELEMENT, PROJECT, TASK AREA & WORK UNIT NUMBERS Project NR-056-578
11. CONTROLLING OFFICE NAME AND ADDRESS Department of the Navy Office of Naval Research Arlington, VA 22217	12. REPORT DATE 6-9-82	13. NUMBER OF PAGES 33
	14. MONITORING AGENCY NAME & ADDRESS (if different from Controlling Office)	15. SECURITY CLASS. (of this report)
16. DISTRIBUTION STATEMENT (of this Report) Approved for public release: distribution unlimited		15a. DECLASSIFICATION/DOWNGRADING SCHEDULE
17. DISTRIBUTION STATEMENT (of the abstract entered in Block 20, if different from Report)		
18. SUPPLEMENTARY NOTES Preprint; in press, Journal of Physical Chemistry		
19. KEY WORDS (Continue on reverse side if necessary and identify by block number)		
20. ABSTRACT (Continue on reverse side if necessary and identify by block number) Platinum, supported on TiO ₂ , TiO and Ti ₂ O ₃ in various forms, has been investigated using a variety of physical and chemical techniques. On H ₂ pretreated TiO ₂ , on TiO and on Ti ₂ O ₃ samples (all platinized), SMSI behavior, i.e. limited H ₂ uptake, was noted. Very fast H-for-D exchange rates were observed for H ₂ D ₂ mixtures on all these materials indicating that dissociative adsorption still occurs readily. Using XPS, SAES, TEM and STEM data we conclude that surface contamination, diffusion of Pt into the bulk oxide, formation of		

DD FORM 1473
1 JAN 73

EDITION OF 1 NOV 65 IS OBSOLETE
S/N 0102-014-6601

SECURITY CLASSIFICATION OF THIS PAGE (When Data Entered)

Block 20. Continued.

surface mixed metal oxides and metal agglomeration are not significant contributors to the observed loss of H_2 uptake capacity. On the basis of qualitative bulk electrical conductivity data and XPS data, we suggest that the SMSI effect is best understood in terms of a bulk oxide reduction model. In this model, bulk conduction band electrons tunnel readily through a thin TiO_2 layer at the surface to reach Pt particles where they are trapped and furnish a negatively charged Pt particle with good capacity for dissociating H_2 but weak binding of atoms.

5 10 8 2
106
RESEARCH

J. Phys. Chem. (in press)
5/82.

2

ABSTRACT

Platinum, supported on TiO_2 , TiO and Ti_2O_3 in various forms, has been investigated using a variety of physical and chemical techniques. On H_2 pretreated TiO_2 , on TiO and on Ti_2O_3 samples (all platinized), SMSI behaviour, i.e. limited H_2 uptake, was noted. Very fast H-for-D exchange rates were observed for H_2 - D_2 mixtures on all these materials indicating that dissociative adsorption still occurs readily. Using XPS, SAES, TEM and STEM data we conclude that surface contamination, diffusion of Pt into the bulk oxide, formation of surface mixed metal oxides and metal agglomeration are not significant contributors to the observed loss of H_2 uptake capacity. On the basis of qualitative bulk electrical conductivity data and XPS data, we suggest that the SMSI effect is best understood in terms of a bulk oxide reduction model. In this model, bulk conduction band electrons tunnel readily through a thin TiO_2 layer at the surface to reach Pt particles where they are trapped and furnish a negatively charged Pt particle with good capacity for dissociating H_2 but weak binding of H atoms.

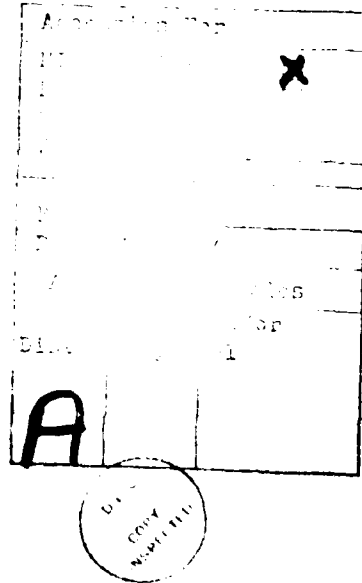
Properties of Pt Supported on Oxides of Titanium^(a)

Cor-Her Chen^(b) and J. M. White^(c)

Department of Chemistry
University of Texas

Austin, TX 78712

- (a) Supported in part by the Office of Naval Research.
(b) Permanent address: Department of Chemistry, Tamkang University, Tamsui, Taipei 251, Taiwan, R.O.C.
(c) Author to whom correspondence should be addressed.



1. INTRODUCTION

The use of transition metal/titania systems has recently received considerable attention in two areas--photoassisted reactions at the gas-solid or liquid-solid interface and strong metal support(SMSI) interaction phenomena. As part of our continuing research on photoassisted reactions⁽¹⁾, we have undertaken work to characterize the substrates we have been using in an effort to understand the role of SMSI effects. This paper reports part of that work.

The SMSI effect, which is characterized by a strongly reduced uptake of hydrogen and carbon monoxide on supported transition metals, (2) has recently drawn intense attention because of promising potential in controlling the activity and selectivity of catalysts. (3-5) The alteration of catalytic properties through interactions with the substrate is a very interesting approach to the development of promising catalytic materials for both conventional and photoassisted heterogeneous reactions.

In this paper we report studies of platinumized oxides of titanium, including various forms of TiO_2 , TiO and Ti_2O_3 . A variety of bulk and surface measurements are reported which provide some clarification of the nature of the interactions between platinum and the oxide supports.

2. EXPERIMENTAL

The TiO_2 (reagent grade anatase, $< 125 \mu m$ diameter particles) was obtained from MCR. Ti_2O_3 and TiO powders (99+% optical grade) were obtained from Alpha Products. Chloroplatinic acid, H_2PtCl_6 , was prepared by dissolving Pt foil (99.99%) in aqua regia. Research grade H_2 and D_2 (98%) were obtained from Linde. Both were purified by passage through a 5A molecular sieve trap immersed in liquid nitrogen.

Two types of anatase were used as support materials: (1) as received from the manufacturer and (2) an H_2 pretreated sample prepared by reducing the above anatase in flowing H_2 (30 ml/min) at $875^\circ C$ for 6 hr and denoted as $TiO_2(H_2 \text{ pre})$.

One set of 2 wt.% Pt catalysts was prepared by impregnating all the support powders with 0.1 N H_2PtCl_6 solution. A second set was prepared by a photodecomposition method. (6) An oxidized form of the $TiO_2(H_2 \text{ pre})$ catalyst was prepared exposing the reduced material to 550 Torr of O_2 at $500^\circ C$ for 17 hr.

Surface areas (H_2 adsorption at 77 K) and H_2 chemisorption measurements were carried out in a standard static volumetric apparatus. For the H_2 uptake measurements, each sample was: (1) degassed for one hr at $200^\circ C$ under dynamic vacuum of 10^{-6} Torr, (2) reduced for 2 hr. with 550 Torr H_2 at $200^\circ C$, (3) degassed again at $200^\circ C$ for one hr., (4) cooled to room temperature under dynamic vacuum and (5) exposed to H_2 for the uptake measurement. For one sample, the temperature in steps (1), (2) and (3) was raised to $400^\circ C$ with no detectable effect on the H_2 uptake isotherm. Therefore, $200^\circ C$ was used routinely.

The H_2 - D_2 isotope exchange studies were carried out in an evacuable, circulation-pumped system (230 ml volume) which was connected to a mass

Atomic composition ratios were calculated from peak-to-peak height ratios and tabulated atomic sensitivity factors.

spectrometer for reaction product analysis. The catalyst was spread uniformly on one face of a quartz reaction vessel (used in related photoassisted reactions) which was part of the circulation loop. In each exchange experiment, 1:1 Torr of an equimolar H_2 - D_2 mixture was dosed into the reactor loop from a connected storage vessel.

Qualitative electrical conductivity measurements were made by pressing the powdered catalyst in a pellet die under 10,000 psi for 5 min. The electrical resistance of the pellet was determined by measuring the current through the pellet-die assembly when a fixed voltage was applied. The thickness and the cross-section of the pellet were measured so that the specific electrical conductivity could be calculated. These measurements have been used only for qualitative guidance.

The X-ray powder diffraction patterns were obtained with a conventional diffractometer (Phillips). The SEM studies utilized a model 634-350, JEM system and the TEM and STEM measurements were done on a JEM 100B system. For the TEM study, samples were dispersed on carbon-coated grids using a modified mixture of catalyst and collodion.

X-ray photoelectron spectra (XPS) and scanning Auger spectra (SAES) are taken with two Physical Electronics Industries (PHI) instruments. In the XPS study, the sample pellets were preheated in a reaction chamber attached to the spectrometer vacuum chamber. Conditions could be chosen to anneal or to dose with D_2 before measurements. For these experiments, a 100 or 250 eV lamp was used to flood the sample against a tungsten heater. In cases where no sample heating was necessary, the powders were pressed into pellets. The relative atomic compositions of the surface layers studied by XPS were calculated from the relative peak areas adjusted for atomic sensitivities taken from the PHI handbook. The SAES measurements were made in a background pressure of 3×10^{-9} Torr using a 3 keV electron beam.

1000-1070

(b) H_2 Adsorption Isotherms.

Table I lists a series of isotherms used in this work. Isotherms are shown as the ratio of the dry, oxidized hydrogen treated and oxidized isotherm, and are plotted as shown. As noted above, two platinumization treatments were used; impregnation (imp) and photo-reduction (photo). As a standard for comparison and for measuring the performance of our apparatus, a commercial Pt/TiO₂ sample was also included.

All the hydrogen adsorption isotherms were recorded at room temperature. Representative data are given in Figs. 1(a) and the extent of the uptake at low pressures (0.1-1.0 Torr) is tabulated in Table II. Upon conversion to H_2 curve (a) of Fig. 1 shows a strong chemisorption step while curve (b) does not. These two curves are typical of the kind of results which are observed; separation of Pt on pretreated TiO₂ by either the photo-reduction route or the impregnation route gives a sample which will not chemisorb significant amounts of hydrogen unless it is first oxidized at high temperatures. Curve (b) is data for a platinum sample prepared by the photo-reduction method and, just before the H_2 uptake experiment, was exposed to O_2 at 400°C and then evaluated at the same temperature. Curve (a) is for this same sample but after oxidation at 600°C. The vertical axis of chemisorbed hydrogen is in $\mu\text{mole gm}^{-1}$ of catalyst and corresponds to a H/Pt ratio of 0.27. This is to be compared with a calculated H/Pt ratio of 0.11 based on an average Pt crystallite size of 170Å (STEM measurement described below) and the assumption of hemispherical particles. For reduced catalysts, STEM measurements indicate a slightly smaller particle size.

It is important to note here that strong H_2 chemisorption is also found on Pt/TiO₂ using titania that is neither pre-reduced nor oxidized before the

H_2 chemisorption experiment. This demonstrates that the strong chemisorption noted in the previous paragraph is not the result of clearing off impurities during oxidation.

Curves (c) and (d) of Fig. 1 are for platinumized (by impregnation) samples of Ti₂O₃ and TiO respectively. They show no chemisorption step and follow the same uptake trends with increasing H_2 pressure as the other samples.

The absence of a chemisorption step in the hydrogen uptake is a characteristic feature of XPS(12). However, it is significant to note here that XPS indicates that the surfaces of all of the materials are oxidized to TiO₂. Since the support materials are all exposed to air before platinumization and since the reduced surfaces are relatively easily oxidized as shown by EPR(7), XPS of powdered samples of titanium(III), it is not surprising that the surfaces were all found by XPS to be TiO₂. The implication is that most properties are present when the surface oxide is reduced even when the support layers are fairly oxidized. This will be discussed further below.

Figure 2 shows, as a function of H_2 uptake for the curves in the absence of Pt. As expected there is no chemisorption step; the slowly rising uptake typical of hydrogen on oxides and hydroxides (see what is seen in Fig. 1 for the platinumized forms). The only difference is that the slow uptake is somewhat more extensive in the presence of Pt. This is supported by infrared measurements (see above) to be related elsewhere(10) which show that surface OH is formed upon exposure of platinumized titania to H_2 . We take this to mean that Pt promotes dissociative adsorption of hydrogen even when it is in a state that does not allow a sizeable surface concentration to develop and that migration from Pt to the oxides of titanium occurs, i.e., spillover.

Returning to a consideration of curves (a) and (b) of Fig. 1, we note

that the uptake of hydrogen at 440 Torr corresponds roughly to a coverage of one monolayer over the oxide surface based on a BET surface area of 100 m²/g and a one monolayer concentration of 10¹⁹ atoms/m². The slow hydrogen isotherms shown in Figs. 1 and 2 are reversible. After evacuating the system overnight at room temperature and 10⁻⁶ Torr, reduction with hydrogen gave the same slowly rising uptake curves. The strongly endothermic oxidation (10 probe/jm in Fig. 1a) should be completely recovered by oxidizing the catalyst to 400°C for one hour. A significant fraction, but certainly not all, of it was desorbed by heating at 400°C for one hour and the desorption was noted during one hour heating at either 100 or 200°C.

The inset of Fig. 2 shows the results of a control experiment with a commercial Pt/A₂O₃ catalyst (Wako having, according to the manufacturer, (1) a dispersion of 0.4%, air results, extrapolated to zero pressure, give 0.37 which we regard as acceptable agreement.

3.2 Catalyst characterization by spectroscopic methods.

X-ray diffraction data are given in Table 1. Prior to the H₂ treatment the X-ray powder diffraction pattern was dominated by rutile peaks at 2θ values of 25.26°, 36.96°, 37.76°, 38.56°, and 48.10° and no rutile peak were found. After reduction, rutile peaks appeared at 27.4°, 36.7°, 38.2°, 41.5° and 44.0°. Even though these samples were dominated by rutile, we note that samples dominated either by rutile or anatase show strong hydrogen chemisorption provided the substrate is oxidized. For example, Pt/TiO₂ formed from reduced TiO₂ is dominated by anatase and shows the same hydrogen uptake as a heavily reduced Pt/TiO₂ that is reoxidized (dominated by rutile). Additional peaks, which we attribute to Ti₉O₁₇ appear in the spectra for samples 2 and 4, i.e. at 26.64°, 28.18°, 35.16° and 35.86° (not resolved). Upon oxidation, these Ti₉O₁₇ peaks disappear.

Small peaks due to Pt crystallites were observable for all of the platinumized samples. Judging from the intensity and apparent widths of these

peaks, it is evident that the loading is 2 wt% Pt in each case, we conclude that some platinum may exist in oxidizing the Pt/TiO₂. The Pt peaks in samples 9 and 11 indicate deposition somewhat higher than for the samples containing TiO₂.

It is important to note that the light blue color and the X-ray peaks due to bulk Ti₉O₁₇ which appear when TiO₂ is treated with H₂ are very stable in room temperature air and upon platinumization either by oxidation or photo-reduction. Oxidation (550 Torr O₂, 100°C, 1 hr) readily removes the Ti₉O₁₇ X-ray peaks but also removes the blue color; in the absence of Pt the sample becomes white while in the presence of Pt it becomes golden brown. The former color is that reported to arise when Ti₉O₁₇ is formed, and the latter is characteristic of oxidized Pt.

EXAFS measurements on the Pt/TiO₂ by photo-reduced Pt (and by the photo-oxidation and re-reduction methods) indicate a broad range of Pt crystallite sizes from 10 to several thousand Å. EXAFS measurements show similar results. Particle sizes estimated as Pt was made by using dispersion X-ray diffraction. These together with the EXAFS data show that the particles are distributed as stated. The average particle size is estimated as 100 Å and the distribution of the particles by the method is, at most, only slightly higher than with the re-reduction method.

EXAFS measurements indicate that oxidizing the Pt/TiO₂ (for example, sample (b) of Fig. 1, as reported by very little change in the Pt particle size distribution. EXAFS measurements on the same sample were inconclusive because the contrast between Pt and the oxide was very poor.

X-ray photoelectron spectra (XPS) were taken to identify the surface composition and chemical environment. Six samples were investigated: (1) TiO₂ (anatase), (2) Pt/TiO₂ (H₂ red), (3) oxidized Pt/TiO₂ (H₂ red), (4) Pt/TiO₂, (5) Pt/TiO and (6) Pt/A₂O₃. Some of these were examined after reduction in H₂ for 2 hr at either 200 or 500°C in the photoelectron

spectroscopy reaction chamber. Additional work is needed to examine the Pt/TiO₂ and Pt/TiO₃ samples.

The results, summarized in Table 2, indicate a relatively large amount of surface carbon is present in every case although the Pt/TiO₂ is somewhat smaller than the Pt/TiO₃ and Pt (non-SMSI) samples. This surface carbon, which we were unable to reduce significantly by pretreatment in the reaction chamber, did not interfere with hydrogen chemisorption on the Pt/Al₂O₃ and oxidized Pt/TiO₂ (H₂ pre) samples. Moreover, samples using TiO₂ and TiO₃ which have smaller relative amounts of surface carbon (based on SMSI results and probably due to overnight purging before taking spectra), show very little chemisorption of hydrogen at low pre cover. This evidence is consistent with notion that the presence of surface carbon is not correlated with H₂ chemisorption. We take this to mean that most of the carbon is on the oxide support.

Other possible poisons, including sulfur, phosphorus and chlorine, may also be ruled out as controlling the nature of the H₂ absorption in these experiments. This is supported by the XPS data for which both the oxidized and not oxidized Pt/TiO₂ (H₂ pre) samples show none of these species but their H₂ chemisorption properties are very different.

The binding energies shown in Table 2 are all referenced to the C(1s) signal which was set at 284.6 eV after initial calibration using the Au(4f_{7/2}) peak at 81.8 eV. The carbon 1s binding energy was first determined as 284.6 eV using a pellet of titania coated with carbon-containing material as a result of pressing it with paraffin paper on the die faces. In the absence of this carbon XPS gave a much lower C(1s) intensity at the same BE.

The Ti(2p_{3/2}) BE's listed in Table 2 all lie within a 1 eV region and the shifts do not correlate with SMSI behavior. For example, the BE of the surface Ti(2p_{3/2}) is 458.9 eV for both Pt/TiO₃ (catalyst F) which shows the

SMSI property and for oxidized Pt/TiO₂ (H₂ pre) (catalyst B) which does not show the SMSI property. The bulk of all the TiO₂ and TiO₃ samples is definitely dominated by Ti⁴⁺ and Ti³⁺ respectively (XPS data) while the surface is oxidized to Ti⁴⁺. Sayre and Armstrong (22) reported that the binding energy shift, $\Delta BE = 0.10 \text{ eV} (\text{TiO}_2/\text{TiO}_3)$, depends on the oxidation state of Ti but is nearly independent of the particular form of the titanium oxides. They find for TiO₂ samples, $\Delta BE = 0.15 \pm 0.4 \text{ eV}$, while for TiO₃ and TiO samples, the values are $0.14 \pm 0.4 \text{ eV}$ and $0.07 \pm 0.3 \text{ eV}$, respectively. Our results give $\Delta BE = 0.13 \pm 0.2 \text{ eV}$ for platinumed catalysts with and without SMSI property (B to H, Table 2) indicating that there are no detectable Ti²⁺ or Ti³⁺ species present on the surface of these Pt catalysts because the SMSI property. We conclude that there is no relationship between the SMSI effect and the oxidation state of the detectable surface Ti ions.

High resolution XPS spectra (25 eV pass energy) with an analyzer resolution of $\Delta E = 0.4 \text{ eV}$ of catalysts with (E, F and H) and without (B) the SMSI property are shown in Fig. 3. The peak positions and half-widths are given in Table 2. Reduction does not lead to a significant increase in FWHM of the Ti(2p_{3/2}) peak; rather a decrease from 1.83 to 1.44 eV is found as indicated in Table 2, samples B and C. Thus, there is no evidence for mixed Ti states upon reduction. We attribute the linewidth variations to changes in surface heterogeneity.

Figure 4 shows XPS for the Pt(4f) region of materials with (E, F and H) and without (B) SMSI behavior. The BE's range from 70.5 to 71.1 eV with no correlation with the SMSI property. Catalyst F, with SMSI, has a Pt(4f_{7/2}) BE of 70.9 eV while catalyst B, non-SMSI, has a peak at 71.1 eV.

The surface atomic Pt/Ti ratios calculated from the XPS peak areas are also listed in Table 2. The results indicate that the SMSI property is not due to diffusion of Pt into the subsurface during reduction. Materials with SMSI behavior (C, E, F and H) show Pt/Ti between 0.06 and 0.36 clearly

indicating that a significant amount of Pt is present on the surface. The results from SAES also confirm this point although their values (Table 2, Catalysts I and J) are somewhat different from the XPS results. Comparing B and C in Table 2 shows that the Pt/Ti ratio does decrease from 0.11 to 0.07 upon reduction at 500°C but this loss cannot account for the total depression of measurable H₂ chemisorption that is observed. In fact, the observed loss is almost within the limits of our ability to detect a significant change in the surface Pt concentration. With reduction, changes in surface morphology (roughness) and changes in surface contamination can account for the observed Pt/Ti variations.

3.3 H₂-D₂ Isotope Exchange.

The results of exposing the catalyst to an equimolar mixture of hydrogen and deuterium are summarized in Table 3 using a concentration function in the form of the equilibrium constant. As thermodynamic equilibrium is approached, the value of this function will increase. The values were calculated from mass spectrometric peak heights assuming no difference in sensitivity among the isotopic forms of molecular hydrogen.

The results are very informative in the sense that none of the Pt-free substrates shows much activity for the exchange. On the other hand, all of the platinumized catalysts exhibit very rapid exchange and the rate of approach to equilibrium is at least as fast for the Pt/Ti₂O₃ (H₂ pre, photo) as it is for the unreduced Pt/TiO₂. Even though the former shows no chemisorption, while the latter does, both readily catalyze the H-for-D exchange reaction. We take this as evidence for the ready dissociation of hydrogen by Pt on both samples with a much more rapid desorption on the former. The same kind of process is proposed to account for the relatively rapid isotope exchange on both Pt/TiO and Pt/Ti₂O₃ neither of which shows any measurable chemisorption of hydrogen at room temperature. The observation of rapid isotope exchange also supports the conclusion drawn in section 3.2 that the relatively large amounts of surface carbon detected by XPS are located primarily on the oxide support and do not interfere with hydrogen adsorption at Pt sites.

It is important to consider the possibility that the exchange reaction is catalyzed by a small number of Pt sites in contact with TiO₂, i.e. only a small fraction of the total amount of Pt is active for the dissociation of H₂. If this is the case, then the observed exchange rate per site is extremely fast and exceeds the rate on Pt which shows strong chemisorption of hydrogen. Although we do not favor this model, it is a possibility if

the interaction between Pt and the underlying TiO_2 activates certain of the Pt atoms.

3.4 Electrical Conductivity Measurements.

The results for electrical conductivity and surface area are summarized in Table 3. The starting material (A) has a specific electrical conductivity of less than $2 \times 10^{-11} \text{ ohm}^{-1} \text{ cm}^{-1}$. This increases by more than two orders of magnitude after heating in hydrogen for 17 hr at 875°C, sample C. Sample B is the same material as C except it was carried through the photoplatinization procedure without using any H_2PtCl_6 in the solution. Platinization of C gives a sample D which has lower specific electrical conductivity, $4.7 \times 10^{-10} \text{ ohm}^{-1} \text{ cm}^{-1}$. Our reproducibility is about $\pm 20\%$, compare D and E, so this change is significant. Comparing the pairs F, G and H, I, indicates that platinization reduces the specific electrical conductivity of TiO and Ti_2O_3 samples by about one order of magnitude. We attribute these decreases to electrons being tied up at surface Pt particles, or species attached to the Pt, thereby decreasing the conduction electron density. With these measurements alone, we cannot rule out the possibility that conductivity changes are the result of variations in either particle-particle contact resistance or charge localization at species chemisorbed on Pt. However, taken with the other data presented here, an internally consistent model involves localization of charge on Pt particles when the underlying oxide is reduced.

4. DISCUSSION

As noted above, the H_2 uptake data, the XRD patterns, the isotope exchange rates, the XPS and SAES data, the electron microscopy results and the electrical conductivity data are all consistent with a model in which the SMSI behavior is dependent upon the ability of the support to donate electrons to the Pt particles. We discuss here in more detail our views about the requirement of bulk reduction in order to observe SMSI and why catalysts which do not accumulate significant coverages of dissociated hydrogen nevertheless exchange hydrogen isotopes very rapidly.

The inability to detect measurable amounts of Ti^{2+} or Ti^{3+} species by XPS on TiO , Ti_2O_3 or $\text{TiO}_2(\text{H}_2 \text{ pre})$ surfaces exposed to air at room temperature (Section 3.2), all of which show SMSI behavior, suggests that electron transfer occurs from reduced subsurface regions to Pt crystallites through a thin barrier layer of TiO_2 . Without significant bulk conductivity, it is difficult to explain the observed effects in terms of Pt- Ti^{n+} metal-metal bonds ($n < 4$) because the surface is oxidized before the Pt is deposited. Consequently, differences in the subsurface (bulk) regions of these materials may play a key role. This bulk conductivity model correlates the SMSI and electrical conductivity data quite well, particularly when we keep in mind the XRD and XPS results. The electrical conductivity decreases in $\text{TiO}_2(\text{H}_2 \text{ pre})$, Ti_2O_3 and TiO when platinized while it increases in TiO_2 . The SMSI effect follows the same pattern.

Using ESR to detect Ti^{3+} , Huizinga and Prins (13) studied the surface reduction of Pt/ TiO_2 at 300°C and 500°C finding reversibility at the lower but not the higher temperature. They attribute this to the formation of microcrystals of Ti_4O_7 formed at the higher temperature as the result of dehydration. Since SMSI behavior is observed after 500°C, but not 300°C, reduction (2), we infer that local low temperature surface reduction of

titania by spillover of H to form Ti^{3+} and OH^- is not the source of the SMSI behavior. The irreversible formation of Ti_4O_7 or Ti_9O_{17} microcrystals (i.e. bulk reduction) at the higher temperatures is consistent with the ESR data and the observed SMSI character. Huizinga and Prins (13) suggest that the appearance of these crystallites near the surface leads to morphological and electronic structure changes in the Pt particles as proposed by others (2,14). In related work, Apple et al. (15) report that strong H_2 chemisorption is found by NMR for Ru/TiO_2 catalysts with both large and small ESR signals due to Ti^{3+} . Since, for their conditions, surface reduction would dominate, we infer that the presence of significant surface Ti^{3+} concentrations does not guarantee SMSI behavior. Our results are also consistent with a model requiring more than surface Ti^{3+} . Indeed, recent ESR work in our laboratory (16) shows that the SMSI property is correlated with the presence of bulk Ti^{3+} signals that are not subject to reversible formation/removal upon exposure/evacuation of H_2 at around room temperature.

The isotope exchange and H_2 uptake data suggest that the dissociative reaction probabilities are about the same on SMSI and non-SMSI catalysts. The heats of adsorption are, however, significantly different, the SMSI catalysts having lower values. A more quantitative description could be developed using a Langmuir isotherm formulation but our data does not permit a quantitative evaluation. Figure 5a shows schematically how H_2 interacts with a Pt catalyst which does not exhibit SMSI. There is a small activation energy, E_{a1} , for dissociative adsorption and a rather large activation energy, E_{d1} , for desorption. The high value of the latter favors a high surface coverage at equilibrium and temperatures near 25°C. Rapid isotope exchange in the H_2 - D_2 equilibration is the result of high surface coverages compensating partially for the relatively high activation energy of desorption. In the SMSI case, Fig. 5b, the activation energy for dissociative adsorption, E_{a2} , is assumed to be about equal to E_{d1} but the

heat of adsorption, E_{a2} , is taken to be much smaller than E_{d1} . Here, low hydrogen coverages at equilibrium are expected, as observed. The unfavorable effect of low hydrogen coverage on the isotope exchange rate is compensated by the low energy required for desorption. In fact, we should not be surprised to find exchange rates proceeding more rapidly on the SMSI materials; the lifetime of a hydrogen atom on the surface is shorter but the dissociative adsorption probability at zero coverage is about the same with the model of Fig. 9. Consequently, the steady state rate of adsorption, and the rate of exchange, will be more rapid for the SMSI case.

Shorter residence times for H atoms on SMSI surfaces have been proposed by Tauster et al. (17) to account for the higher activity and selectivity of Ni/TiO_2 as compared with Ni/SiO_2 or Ni/Al_2O_3 , for Fischer-Tropsch synthesis. The model of Fig. 5 can account for these differences. The shorter lifetime is beneficial to higher activity so long as it is long enough to allow the reaction of interest to compete effectively with other reactions.

In agreement with Baker et al. (14), who used TEM, our results using XRD and TEM indicate that SMSI is not the result of agglomeration of Pt during various treatments. Neither surface impurity poisons nor diffusion of Pt into subsurface regions are significant contributors to the SMSI effect according to our XPS, H_2 uptake and H_2 - D_2 exchange results.

Tauster et al. (17) have suggested that the degree of SMSI effect reached depends upon the ease with which the metal oxide is reduced to provide electron rich cations at the surface which form metal-metal bonds with deposited Group VIII metals like Pt. Our results are consistent, in part, with this model. However, we favor a model in which attention is focussed on the reduction of the bulk which supplies electrons to the adsorbed Pt and lowers their ability to bind atomic hydrogen. A slight change in the language, will bring the two models into agreement. In

selecting materials for an SMSI effect, we propose choosing a support with relatively high electrical conductivity and a work function lower than the deposited metal. To achieve n-type electrical conductivity in typical metal oxides, reduction to remove lattice oxygen must be carried out. The more readily this occurs, the stronger the SMSI effect. By reduction, not only is the conductivity changed, the work function also decreases as the Fermi level moves toward the bottom of the conduction band. For charge transfer from support to Pt upon platinization, the work function of the support must be smaller than that of the metal, i.e. the highest occupied levels of the support lie above the highest occupied levels of the Pt before contacting the two. Materials with low conductivity will not show SMSI unless dopants supplying charge carriers to the conduction band are introduced.

Although p-type semiconductors can be included in this description, electron transfer to Pt from the support will require a "hopping" scheme from one acceptor site to another. Consequently, relatively high doping, to bring these sites close enough for orbital overlap, is required. For n-type material, the conduction band is utilized, so all one needs is thermal excitation into the conduction band and tunneling through the contact barrier at the support/metal interface, i.e. at the TiO_2/Pt junction.

Supporting evidence based on electrical conductivity and type of charge carrier is given in Table 4. We agree completely with Tauster et al. (17) in considering the oxides which show SMSI; however, our description is somewhat broader and includes materials which are not easily reduced. For example, SiC is not in the oxide category and is not readily reduced. (18) In a separate study, (19) we have found SMSI behavior for Pt/SiC and an increased H_2 - D_2 exchange rate upon platinization. This is consistent with our model and suggests that metal-metal bond formation is not a necessary condition for observing SMSI behavior.

Other H_2 uptake studies (20) also support the importance of the bulk

electrical conductivity and Fermi level position in SMSI. For example, no SMSI property is observed for the Pt/ TiO_2 system if the titania is pretreated in flowing H_2 for 6 hr at 700°C and then platinized. As in the work reported here, we expect the surface to reoxidize during platinization and/or exposure to air. The absence of SMSI then suggests that the reduction process did not increase the bulk conductivity sufficiently and/or did not raise the Fermi level of the titania to a value high enough to permit charge transfer. Note that the work functions of undoped TiO_2 and Pt are 6.2 eV (21) and 5.7 eV (22), respectively.

We have also observed electron transfer from Pt to rutile by measuring the electrical properties (I, V, R and C) of a thin film of Pt deposited on single crystal rutile, pretreated in flowing H_2 for 1 hr at 500°C. (19)

The bulk effect charge transfer model suggested here is not new. Baddour and Delbert (23) proposed a similar model in 1966 to explain the promotion of Ni supported on Ge in the catalysis of formic acid decomposition. In another important contribution, Solymosi (24) has reviewed the catalytic importance of the electrical properties of supports. The implication of the bulk conductivity model for electron transfer is that as the metal crystallite or cluster size becomes smaller, the surface charge density will increase. This may account for the different catalytic behavior and the observed resistance to sintering for smaller particles. (25) Our model emphasizes the importance of electron transfer from the bulk of the support to the metal as the key for SMSI behavior. Electron transfer through interfacial metal-metal bonds or through tunneling, as described above, can result in SMSI effects. The negatively charged metal particles will tend to increase their surface areas to reduce their surface charge densities. The expected morphological changes have been observed by Baker, et al. (14) who found a tendency towards flatter pill-box Pt structures when Pt/ TiO_2 was reduced at elevated temperatures.

Prior to reduction or after oxidation, the Pt particles had hemispherical shapes. We have found similar morphology differences; (26) Pt/TiO₂ shows hemispherical Pt particles, Pt/TiO₂^(1/2, PrO) shows polyhedral particles, and Pt/TiO shows raft-like particles.

One SMSI support which appears to fall completely outside the proposed selection rule is MnO; the reason is not clear, but it is worth noting that nonstoichiometric MnO is a semiconductor(27) while, in stoichiometric form it is an insulator.(17,28) Further study is required to clear up this question.

Speculation about the formation of mixed metal oxides in SMSI systems is not warranted here but it does deserve additional study. However, we note that the formation of mixed metal oxides typically requires an oxidizing environment in excess of 500°C. In order to avoid their formation and the possibility of significant impurity and/or diffusion of metal catalyst into the bulk of the support(29,30), our catalysts never encounter a temperature higher than 500°C, during or after platinization, so such mixed metal oxide effects are not likely to contribute significantly.

ACKNOWLEDGMENTS

The authors would like to express their hearty thanks to Dr. Marvin Deviney and Dr. Paul Buccemi for their kindness in taking most of the TEM and STEM micrographs for us. Thanks are also extended to Miss L. J. Fu for her assistance in running the SMS and Mr. Shiu-Min Fang for his assistance in making electrical conductivity measurements.

REFERENCES

1. a. S. Sato and J. M. White, *J. Phys. Chem.*, **85**(1981)592.
b. S. Sato and J. M. White, *J. Catalysis*,
2. S. J. Tauster, S. C. Fung, R. L. Garten, *J. Am. Chem. Soc.*, **100**(1978)170.
3. a. M. A. Vannice and R. L. Garten, *J. Catal.*, **56**(1979)236.
b. M. A. Vannice, S. H. Moon, C. C. T'wu, *Am. Chem. Soc., Div. Pet. Chem. preprints*, **25**(1980)303.
4. M. A. Vannice, *J. Catal.*, **50**(1977)228.
5. M. A. Vannice, S. H. Moon, S. Y. Wang, paper presented at American Chemical Society National Meeting, Houston, March 1980.
6. B. Kraeutler and A. J. Bard, *J. Am. Chem. Soc.*, **100**(1978)1694.
7. P. C. Gravelle, F. Juillet, P. Meriadeau and S. J. Teichner, *Disc. Faraday Soc.*, **52**(1971)140.
8. Powder pellets of TiO and Ti₂O₃ have been examined in our laboratory by John Schreifeis and Bor-Her Chen.
9. John Schreifeis, R. L. Hance, D. N. Beiton, Bor-Her Chen and J. M. White, in preparation.
10. Katsumi Tanaka and J. M. White, *J. Phys. Chem.* (to be submitted).
11. Technical Service Department, Matheson Coleman & Bell Company, Cincinnati, Ohio.
12. C. N. Sayers and N. R. Armstrong, *Surface Sci.* **77**(1980)301.
13. T. Huizinga and R. Prins, *J. Phys. Chem.* **85**(1981)2156.
14. R. T. K. Baker, E. B. Prestridge and L. Garten, *J. Catal.*, **59**(1979)293.
15. T. M. Apple, P. Gajardo and C. Dybowski, *J. Catal.* **68**(1981)103.
16. B.-H. Chen and J. M. White, unpublished data.
17. S. J. Tauster, S. C. Fung, R. T. K. Baker, J. A. Horsley, *Science*,

21(1981)1121.
 18. E. A. Gulbranson and S. A. Jansson, Proc. Int. Congr. Met. Corros., 5th(1979)293.
 19. Bor-Her Chen and J. M. White (in preparation).
 20. S.-M. Fang, B.-H. Chen and J. M. White, J. Phys. Chem. (in press).
 21. V. S. Fomenko, "Emission Properties of Elements and Chemical Compounds", Handbook (in Russian) Izd. Akad. Nauk Ukr. SSR (1965).
 22. J. E. Demuth, Chem. Phys. Letters, 45(1977)12.
 23. R. F. Baddour and M. C. Reibert, J. Phys. Chem., 70(1966)2173.
 24. F. Solymosi, Catal. Rev., 1(1967)233.
 25. R. T. K. Baker, E. B. Prestridge and R. L. Garten, J. Catal., 56(1979)390.
 26. B.-H. Chen, J. M. White, M. L. Deviney and L. R. Brostrom, (to be submitted).
 27. M. Leblanc and H. Sachse, Z. Physik, 32(1931)887.
 28. C. N. R. Rao and G. V. Subba Rao, Phys. Stat. Sol.(A) 1(1970)597.
 29. C. C. Kuo, S. C. Tsai, M. K. Bahl and Y. W. Chung, Surface Sci., 95(1980)1.
 30. B. J. Tatarchuk and J. A. Dumesic, J. Catal. 70(1981)308.
 31. G. V. Samsonov, The Oxide Handbook, Plenum(New York, 1973).

Table 1. Summary of the Properties of Representative Samples.

Sample	H ₂ uptake (mmole/gm)	Dispersion H ₂ /O ₂ Exchange	X-ray Powder Data	Average Pt Particle Size
1. TiO ₂	0	--(a)	inactive	Ana (b)
2. TiO ₂ (H ₂ pre)	0	--	inactive	Ana, Rut, Ti ₉ O ₁₇
3. Pt/TiO ₂ (imp)	10	0.20	active	Pt, Ana, Rut
4. Pt/TiO ₂ (H ₂ pre, imp)	0	--	active	Pt, Ana, Rut, Ti ₉ O ₁₇
5. Oxidized Pt/TiO ₂ (H ₂ pre, imp)	10	0.20	active	Pt, Ana, Rut
6. Pt/TiO ₂ (H ₂ pre, photo)	0	--	active	100 A
7. Oxidized Pt/TiO ₂ (H ₂ pre, photo)	10	0.20	active	>100 A
8. TiO ₂	0	--	inactive	
9. Pt/TiO ₂ (imp)	0	--	active	Pt, TiO ₂
10. TiO	0	--	inactive	
11. Pt/TiO(imp)	0	--	inactive	Pt, TiO
12. 5 wt.% Pt/Al ₂ O ₃	100	0.37	active	Pt, Al ₂ O ₃

Notes: a. (--) in the dispersion column indicates that this parameter can not be determined from hydrogen adsorption.
 b. Ana = anatase, Rut = rutile, pre = pre-reduction, imp = impregnation.
 c. (----) in Pt particle size column indicates that this parameter was not determined.

Table 3. Surface Area, Electrical Conductivity and Isotope Exchange Data

No	Sample	Surface Area (m ²)	Specific Electrical Conductivity (ohm ⁻¹ cm ⁻¹)	25 sec	60 sec	300 sec	Temperature
A	TiO ₂ 0.33 gm	4.55	<2.0 x 10 ⁻¹¹	10 ⁻³ 0.00 0.00	0.006 0.00 0.00	0.017 0.00 0.00	200°C 100°C 25°C
B	TiO ₂ (a*)	3.7 x 10 ⁻⁹					
C	TiO ₂ (a) 0.35 gm	3.85	2.4 x 10 ⁻⁹	2.8 x 10 ⁻³ 0.00 0.00	0.12 0.00 0.00	0.21 0.00 0.00	200°C 100°C 25°C
D	Pt/TiO ₂ (a) 0.35 gm SMSI	3.85	4.7 x 10 ⁻¹⁰	1.20 ± 0.02 1.05 ± 0.05 1.01 ± 0.01	2.8 ± 0.2 2.51 ± 0.03 2.30 ± 0.10	3.31 ± 0.01 3.20 ± 0.02 3.07 ± 0.05	200°C 100°C 25°C
E	Pt/TiO ₂ 0.35 gm	3.85	5.0 x 10 ⁻¹⁰	1.18 ± 0.02 0.82 ± 0.02 0.71 ± 0.01	2.4 ± 0.2 2.0 ± 0.1 1.82 ± 0.01	3.1 ± 0.1 2.97 ± 0.01 2.72 ± 0.01	200°C 100°C 25°C
F	TiO 0.11 gm	3.85	1.2 x 10 ⁻¹	10 ⁻⁴ 0.00 0.00	5.4 x 10 ⁻⁴ 0.00 0.00	1.1 x 10 ⁻² 0.00 0.00	200°C 100°C 25°C
G	Pt/TiO 0.11 gm	3.85	3.4 x 10 ⁻³	1.3 1.1 ± 0.01 0.9 ± 0.1	2.82 ± 0.04 2.61 ± 0.03 2.22 ± 0.03	3.6 ± 0.1 3.49 ± 0.02 3.45 ± 0.02	200°C 100°C 25°C
H	TiO 0.25 gm		6.1 x 10 ⁻³	0.00	Hot Done Hot Done 0.00	0.00	200°C 100°C 25°C
I	Pt/TiO 0.25 gm SMSI		6.2 x 10 ⁻⁴	0.71 ± 0.09	Hot Done Hot Done 2.33 ± 0.02	3.3 ± 0.1	200°C 100°C 25°C

(a) is TiO₂(H₂ pre)

(a*) is TiO₂(H₂ pre) treated using photoreduction conditions but without adding H₂PtCl₆.

No	Sample	Treatment	RE/eV	Surface Atomic Ratio	Minor Surface Contaminant
A	TiO (anatase)	Degassed at 25°C	459.0	0.00	3.12
B	Oxidized Pt/TiO (H ₂ pre)	Degassed at 25°C	459.9 (d)	0.11	3.60
C	Oxidized Pt/TiO (H ₂ pre)	Red. at 200°C	459.3 (2.00)	0.07	3.02
D	Pt/TiO (a)	Red. at 450°C	459.4 (1.44)	0.13	5.75
E	Pt/TiO (H ₂ pre) photo platinumized	Red. at 200°C	458.5 (1.93)	0.06	3.47
F	Pt/TiO (H ₂ pre) photo platinumized	Red. at 200°C	458.9 (1.67)	0.20	3.44
G	Pt/TiO (H ₂ pre)	Red. at 200°C	458.6 (1.55)	0.15	3.20
H	Pt/TiO (H ₂ pre)	Red. at 450°C	458.0 (1.95)	0.36	3.02
I	Pt/TiO (H ₂ pre)	Red. at 200°C	458.0 (1.67)	0.36	3.02
J	Pt/TiO (H ₂ pre)	Red. at 200°C	458.0 (1.95)	0.31	3.42
K	Pt/TiO (H ₂ pre)	Red. at 25°C	458.0 (1.95)	0.31	3.42
L	Pt/TiO (H ₂ pre)	Red. at 25°C	458.0 (1.95)	0.11	2.00
M	Pt/TiO (H ₂ pre)	Red. at 25°C	458.0 (1.95)	0.18	0.18

(a) The pellet was prepared with paraffin paper as described in the text.

(b) Y = Detectable, N = Not detectable.

(c) * = SMSI property (strongly reduced H₂ chemisorption) is known to be present for this material.

(d) Full width at half maximum in eV.

Table 2. Surface composition and XPS Binding Energies.

Table 4.
The correlation of SMSI behavior with electronic properties of supports.

Support Material	Carrier Type	Electrical Conductivity $\text{ohm}^{-1}\text{cm}^{-1}$	SMSI	Reference
TiO	Metal	10^{-1}	Y	a
Ti ₂ O ₃	n	10^{-3}	Y	a
TiO ₂	n	10^{-11}	N	a
Nb ₂ O ₅	n	10^{-1} (200°C)	Y	17
V ₂ O ₃	Metal	10^{+3}	Y	17, 31
HfO ₂	p	10^{-5} (400°C)	N	17, 31
ZrO ₂	p	10^{-5} (400°C)	N	17
Sc ₂ O ₃	p	10^{-7} (650°C)	N	17, 31
MgO	n	10^{-12}	N	17, 31
SiO ₂	Insul ^d	10^{-12}	N	17, 31
Al ₂ O ₃	Insul	10^{-12}	N	17, 31
SiC	Metal	10^{-3}	Y	19

(a) This paper.

(b) Insulator

FIGURE CAPTIONS

Figure 1. H₂ uptake curves for platinumized titanium oxides. (a) oxidized Pt/TiO₂(H₂ pre), ■, (b) Pt/TiO₂(H₂ pre), □, (c) Pt/Ti₂O₃, ▲, (d) Pt/TiO, ●.

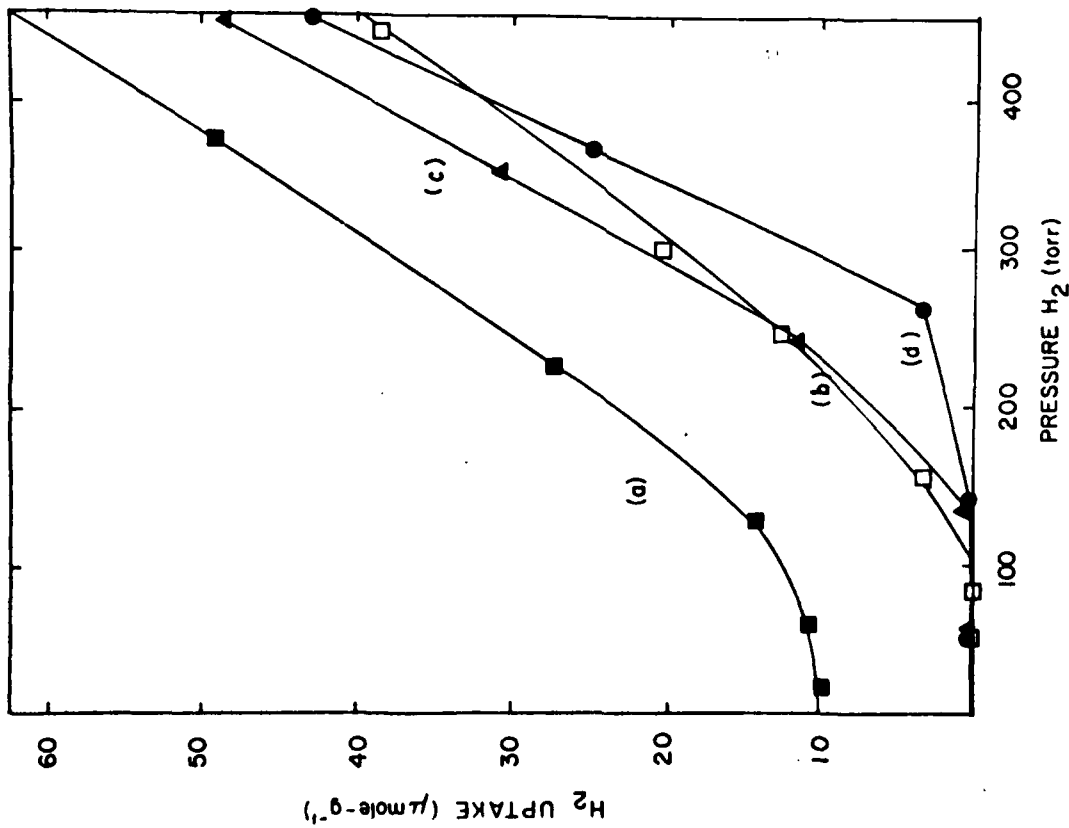
Figure 2. H₂ uptake curves for titanium oxides. ■, TiO₂; □, TiO₂(H₂ pre); ▲, Ti₂O₃.

Insert is H₂ uptake curve for 5% Pt/Al₂O₃ and the axes plot the same variables as the larger figure.

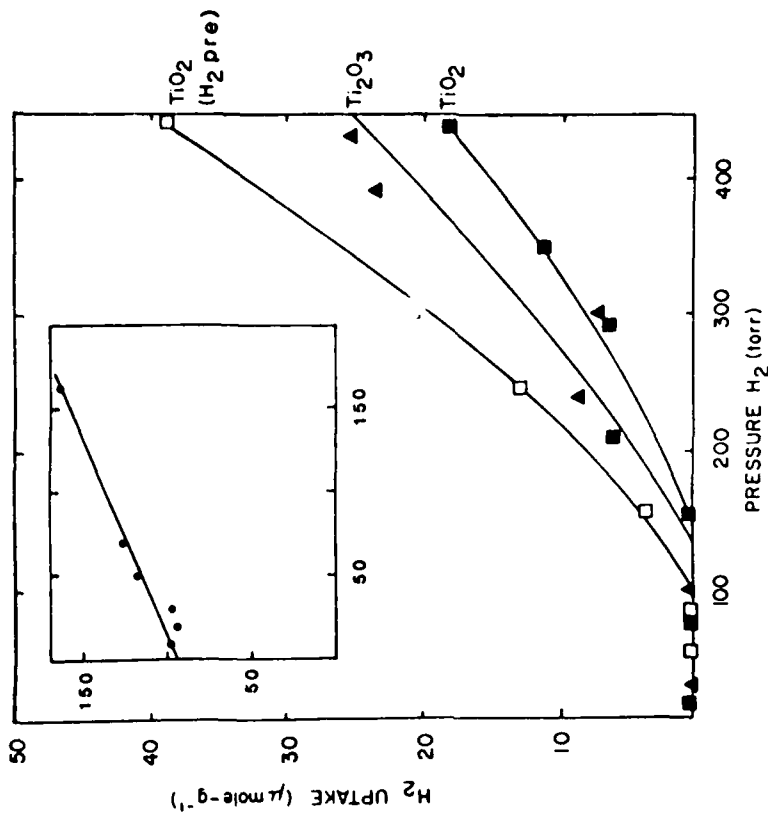
Figure 3. Ti(2p) XPS spectra for some of the systems listed in Table 2. (B) Oxidized Pt/TiO₂(H₂ pre). (F) Pt/Ti₂O₃, H₂ reduction at 200°C. (C) Oxidized Pt/TiO₂(H₂ pre), reduced in-situ at 500°C. (H) Pt/TiO, H₂ reduction at 200°C. (G) Pt/Ti₂O₃, H₂ reduction at 500°C.

Figure 4. Pt(4f) XPS spectra for some of the systems of Table 2. (B) Oxidized Pt/TiO₂(H₂ pre), 50 eV pass energy. (E) Pt/TiO₂(H₂ pre), H₂ reduction at 200°C, 50 eV pass energy. (F) Pt/Ti₂O₃, H₂ reduction at 200°C, 25 eV pass energy. (H) Pt/TiO, H₂ reduction at 200°C, 25 eV pass energy.

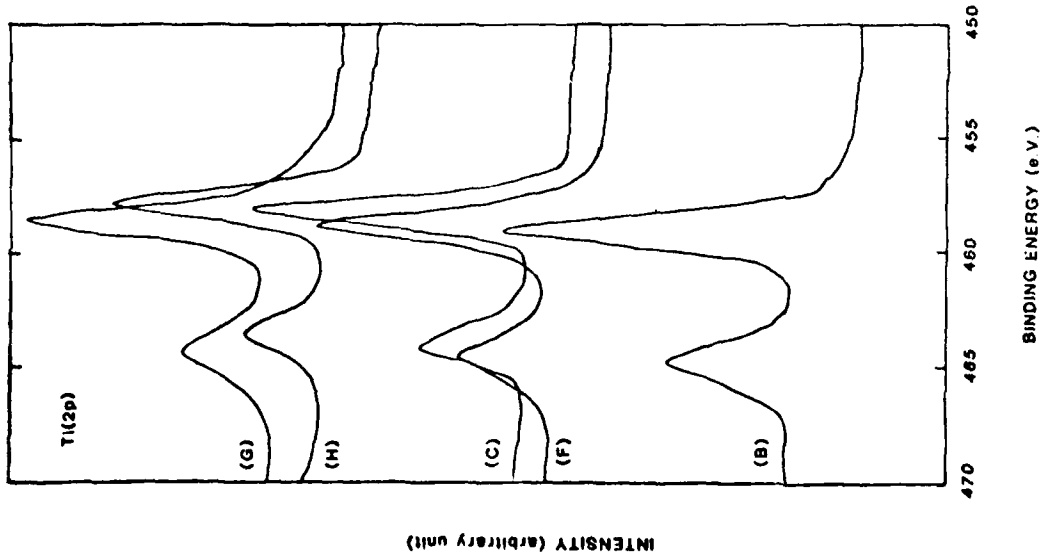
Figure 5. Schematic reaction profiles for H₂ interacting with Pt/TiO₂ systems without, (a), and with, (b), the SMSI property.



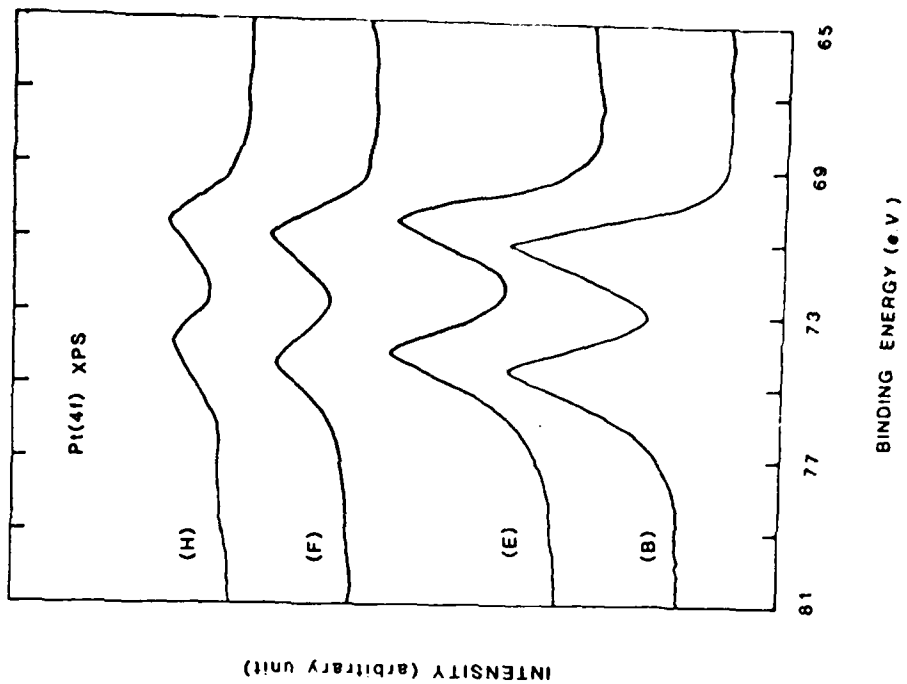
Chem, vol 6 ; fig 1



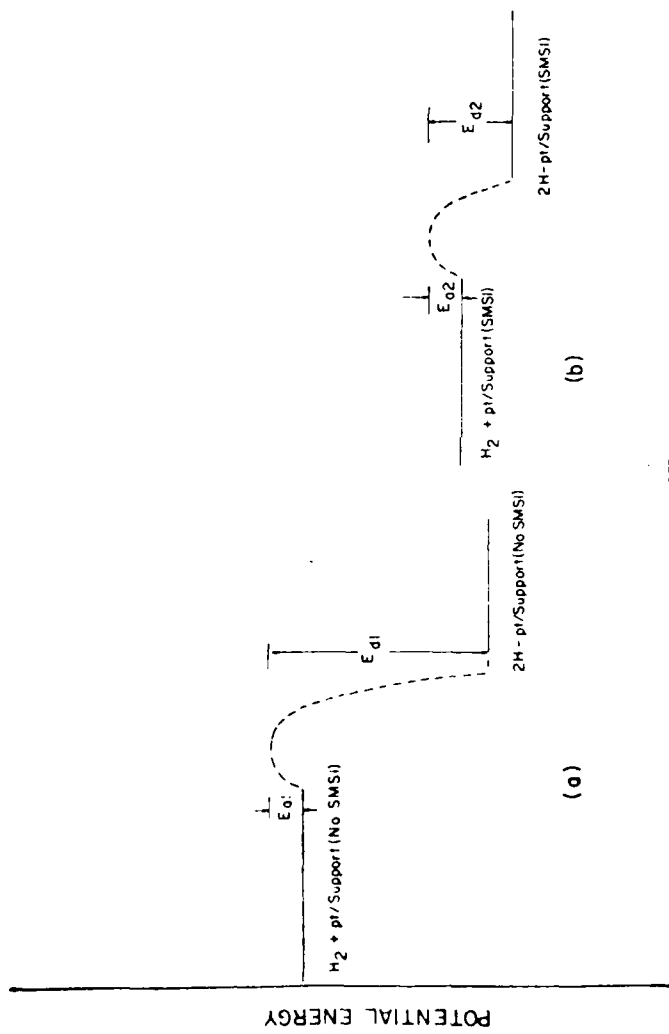
Chem, vol 6 ; fig 2



Chem, white: 733



Chem, white: 73



REACTION COORDINATE

Chem. Write: 7/9/87

END

DATE
FILMED

0-82

DTIC